Development 133, 2596 (2006) doi:10.1242/dev.02461

Identification, emergence and mobilization of circulating endothelial cells or progenitors in the embryo

Luc Pardanaud and Anne Eichmann *Development* **133**, 2527-2537.

The ePress version of this article published on the 25th May contains an error in the author affiliations and in Fig. 2N,O.

The final printed and online versions of the article are correct.

We apologise to the authors and readers for this mistake.

Development 133, 2527-2537 (2006) doi:10.1242/dev.02421

Identification, emergence and mobilization of circulating endothelial cells or progenitors in the embryo

Luc Pardanaud* and Anne Eichmann

Using quail-chick parabiosis and QH1 monoclonal antibody analysis, we have identified circulating endothelial cells and/or progenitors in the embryo. These cells were already present early in ontogeny, before the third embryonic day. Under normal conditions, they integrated into most tissues but remained scarce. When experimental angiogenic responses were induced by wounding or grafts onto the chorioallantoic membrane, circulating endothelial cells were rapidly mobilized and selectively integrated sites of neoangiogenesis. Their mobilization was not dependent on the presence of the bone marrow as it was effective before its differentiation. Surprisingly, mobilization was not effective during sprouting angiogenesis following VEGF treatment of chorioallantoic membrane. Thus, embryonic circulating endothelial cells were efficiently mobilized during the establishment of an initial vascular supply to ischemic tissues following wounding or grafting, but were not involved during classical sprouting angiogenesis.

KEY WORDS: Circulating endothelial cells/Progenitors, Embryo, Quail-chick parabiosis, Mobilization, Bone marrow

INTRODUCTION

The development of the vascular plexus is an essential event during ontogeny and mutations affecting genes involved in the emergence, the differentiation and the maturation of the endothelial system lead to the rapid death of embryos. The primary vascular tree develops by two processes, vasculogenesis and angiogenesis (Risau and Lemmon, 1988), that relate to the intrinsic or the extrinsic origin of endothelial cells (ECs). In the yolk sac, vasculogenesis leads to the differentiation of the hemangioblast (Murray, 1932), a stem cell that gives rise to both ECs and hematopoietic cells (HCs), whereas in the embryo, it leads to the emergence of isolated angioblasts (Sabin, 1920). Angiogenesis involves the development of an endothelial network from preexisting vessels that sprout towards unvascularized regions. Following the development of the primary vascular tree, the plexus is remodeled into arteries and veins, and terminal differentiation is accomplished by the formation of the vascular wall (Carmeliet, 2003).

In the adult, once the definitive vascular network is established, ECs remain essentially quiescent with neovascularization only occurring during physiological or pathological events. For a long time, adult neovascularization was thought to be exclusively achieved by angiogenesis. However, grafting experiments had suggested that circulating ECs (CECs) could participate in neovascularization processes (Stump et al., 1963; Kennedy and Weissman, 1971). CECs have since been isolated and characterized in the adult (Asahara et al., 1997; Shi et al., 1998; Takahashi et al., 1999; Gehling et al., 2000; Lin et al., 2000; Peichev et al., 2000). In vitro, these cells differentiate into ECs; in vivo, they home to sites of neovascularization, including tumoral regions or ischemic territories (Asahara et al., 1999; Cogle and Scott, 2004; Urbich and Dimmeler, 2004a; Urbich and Dimmeler, 2004b). Furthermore, in addition to CECs, adult neovascularization seems to involve circulating endothelial progenitor cells (EPCs) (Urbich and Dimmeler, 2004a; Urbich and Dimmeler, 2004b). EPCs have important potential therapeutic applications, as their administration could stimulate blood vessel growth in conditions of hypo-vascularization (hind limb ischemia, myocardial infarction, stroke, wound healing). Genetic manipulation of EPCs could also allow the inhibition of blood vessel growth in conditions of hyper-vascularization (diabetic retinopathy and tumorigenesis).

EPCs have been isolated from mouse embryos and were shown to form tubes in vitro and in vivo (Vajkoczy et al., 2003; Cherqui et al., 2006). However, it remains unknown when and where these cells form during embryonic development. In the quail-chick chimera system (Le Douarin, 1969) and using the QH1 monoclonal antibody, which is specific for HCs and ECs of the quail species, as a marker (Pardanaud et al., 1987), a study showed that the allantois, an avian appendage, produces both ECs and HCs. When a quail allantois was grafted in the coelomic cavity of a chick host, $QH1^+$ECs and HCs colonized chick territories and sometimes reached the host bone marrow. Owing to the distance between the region of graft, the coelom, and the site of colonization, the bone marrow, interstitial migration of $QH1^+$ECs was unlikely. It was postulated that this colonization occurred through the bloodstream (Caprioli et al., 1998). Although these experiments suggested that the allantois could be a site of emergence of CECs/EPCs, the presence of these cells in the circulation and the extent of their participation to the developing vasculature remained to be determined.

We have developed a direct experimental approach to identify CECs/EPCs in developing embryos and to examine their participation to the developing vasculature. Using quail-chick parabiosis, we demonstrate that CECs/EPCs are present in the embryo and can be mobilized during angiogenic processes induced by grafting of organ rudiments on the chorioallantoic membrane (CAM) or by wounding. We also show that: (1) the emergence of these CECs/EPCs occurs early in ontogeny prior to the formation of the allantois, and is thus not restricted to this territory; (2) their mobilization is not dependent on the presence of the bone marrow; and (3) CEC/EPC mobilization does not occur during all angiogenic processes.

INSERM, Unit 36, F-75005, Paris, France and Collège de France, F-75005, Paris, France.

*Author for correspondence (e-mail: luc.pardanaud@college-de-france.fr)

Accepted 2 May 2006

MATERIALS AND METHODS

Embryonic EPC preparation

Quail (*Coturnix coturnix japonica*) paraxial (somites and segmental plates) and splanchnopleural mesoderms were isolated from 2-day-old (E2) embryos (10-23 somite stage) as described (Pardanaud et al., 1996). The tissues were digested with trypsin (Gibco BRL) for 10 minutes at 37°C and washed in phosphate-buffered saline (PBS)/10% newborn calf serum (NCS, Invitrogen) (Fig. 1A). The suspensions were centrifuged and resuspended in 40% chick embryonic extract, 40% PBS and 20% of penicillin-streptomycin (PS, Gibco BRL). The cell number varied between 3×10^3 (six embryos for splanchnopleural mesoderm) to 10^4 cells/μl (11 embryos for paraxial mesoderm).

Embryonic blood cell harvest

Blood was harvested from quail hearts at E3 (*n*=33), E4 (*n*=22) and E5 (*n*=22). E15 quail blood was isolated from a vitelline artery (*n*=8). The blood was transferred to a tube containing PBS, 10% NCS and heparin (Sigma) at 4°C. To separate white and red cells, lympholite M (Cedarlane Laboratories) was mixed V/V with the cell suspension. After centrifugation, a cloud of white cells, present at the interface between the two solutions, was harvested, washed in PBS/NCS, centrifuged and resuspended in PBS/NCS (5×10^3 to 7×10^4 cells/μl).

Intracardiac injections

E2 chick (*Gallus gallus*, JA57) embryos were used (14-23 somite stage). An artificial dark field was made using Indian ink injection under the embryo. The ectoderm and the pericardium were carefully removed with fine tweezers and 1-2 μl of cell suspension were manually injected into the heart (Fig. 1A). The embryos or organs were dissected between 1 and 14 days later.

Parabiosis

E2 chick and quail embryos (13-23 somite stage) were isolated with their yolk sac and placed side by side on semisolid medium (50% agar, 20% PBS, 20% chick yolk, 10% PS) in a 35 mm Petri dish (Fig. 1E). The dishes were incubated 48 hours at 37°C.

Classical parabioses were performed according to Wong and Ordahl (Wong and Ordahl, 1996). The surviving parabioses (244/2045=12%) were sacrificed between E7, when the two CAMs first contacted one another, and E15. Between E7 and E11, blood smears were prepared from chick embryos by sectioning an extra-embryonic vessel. Smears were fixed in 4% paraformaldehyde (PAF, Sigma).

Grafts of cells and organ rudiments

Endothelin 1-producing CHO cells (Parnot et al., 1997) or control cells were cultured in DMEM/Ham's F12, 7.5% fetal calf serum, 1% PS. Cells were isolated with trypsin and placed overnight in hanging drops to obtain dense suspensions (75×10^4 cells/drop), which were deposited on the chick CAM from E9 parabioses. A silicon ring delimited the grafted region. After 1-5 days, the grafted region was fixed in PAF.

E3 quail limb, gut and lung buds, isolated as previously described (Pardanaud et al., 1989), were placed on the chick CAM of E6-9 parabioses and incubated for 1 to 9 days.

A part of chick liver was retrieved from two E15 parabioses and grafted on the CAM of E8 chick hosts in close contact with E3 chick limb or visceral buds. The developed associations and a part of the chick host liver were isolated 6 days later.

Wounding of the wing and CAM

On E13 parabioses, the chick CAM was sectioned and the right wing was exposed on the CAM. Using a microscalpel, a deep longitudinal incision (±5 mm) was made at the level of the ulna. The parabioses were sacrificed after 6 to 48 hours. The two chick wings (wounded and contralateral) were isolated, the feather buds were shortened, and some chick hearts and livers were fixed.

On E8 parabioses, the wound (±1 mm) was made at the level of the digit region. The two wings were fixed 24 hours after the injury.

To wound CAMs, a silicone ring was placed on the chick CAM of E10 parabioses. Using a microscalpel, six to eight venules or arterioles were cut. After 24 hours, the CAM regions were fixed in PAF, Bouin's fluid or in 1.5% ascetic acid in cold absolute ethanol.

VEGF-induced angiogenesis on CAM

Sterile filter papers (1 cm^2, Whatmann 3MM) were dipped in a solution of cortisone acetate (Sigma) in absolute ethanol (3 mg/ml) to reduce inflammation (Brooks et al., 1999). After air-drying, they were placed on the CAM of chick embryos from E10 parabioses. Recombinant human $VEGF_{165}$ (R&D Systems and ABCys) or PBS was applied on the filters (25 μl=2 μg). The parabioses were sacrificed 4 days later; the filter papers together with the CAM areas were removed and rinsed twice in PBS. Under the stereomicroscope, the number of vessel branches was counted, then the filters were removed and CAMs were processed for immunohistochemistry.

BrdU incorporation

One parabiosis on which a limb bud had been grafted on the chick CAM for 9 days, intravenously received 40 μl of BrdU (1000×, Roche Diagnostics). After 4 hours the graft and the chick host heart were fixed in PAF. Sections were stained with a biotinylated mouse anti-BrdU antibody (1/10 in PBS) (Pharmingen) and diaminobenzidine (Sigma). A double staining was performed with QH1 followed by an alkaline phosphatase-conjugated secondary antibody.

Immunohistochemistry

Unless indicated otherwise, all tissues were fixed in Bouin's fluid, dehydrated, embedded in paraffin and sectioned (5-7.5 μm). Sections were deparaffinized then rehydrated in PBS. QH1 (undiluted hybridoma supernatant) staining was visualized using peroxydase- (BioRad), alkaline phosphatase- (Clinisciences), Texas Red- (Southern Biotechnologies), Alexa 488- or Alexa 555-conjugated secondary antibodies (Invitrogen), as previously described (Pardanaud et al., 1996). QH1-GRL2, QH1-LEP100, QH1-LEA double staining was performed on 1.5% ascetic acid-absolute ethanol-fixed sections. QH1-*Sambucus nigra* lectin staining was performed on PAF-fixed sections.

GRL2 (Thomas et al., 1993) is an avian-specific monoclonal antibody recognizing HCs. GRL2 (1/100 in PBS, overnight at 4°C) was revealed by an Alexa 488 goat anti mouse IgG1.

LEP100 monoclonal antibody stains macrophages (Lippincott-Schwartz and Fambrough, 1986). LEP100 (1/5 in PBS, overnight at 4°C) was revealed by an Alexa 555 goat anti mouse IgG.

LEA agglutinin (Lycopersicon esculentum, Sigma) labels macrophages and avian venous endothelium (Navarro et al., 2003). After rehydration, sections were pretreated with 0.025% trypsin at 37°C for 10 minutes. Biotinylated LEA (20 μg/ml in PBS-0.1% triton, overnight at 4°C) was revealed using Cy3 streptavidin (Amersham).

Biotinylated *Sambucus nigra* lectin (Hagedorn et al., 2005) (1/400 in PBLEC buffer-PBS pH6.8, 1 mM $CaCl_2$, 1 mM $MgCl_2$, 0.1 mM $MnCl_2$, 1% triton-, overnight at 4°C) recognizes avian ECs and was revealed using Cy3 streptavidin.

In toto QH1-*Sambucus nigra* lectin double staining was performed on chick CAM rings. After overnight incubation in PBS-3% NCS, 0.5% triton at 4°C, the rings were washed in PBS (3×30 minutes), PBLEC (30 minutes) and biotinylated *Sambucus nigra* lectin (1/100 in PBLEC) was applied overnight at 4°C. After PBS washes, CAM rings were incubated overnight (4°C) in QH1, then stained with Cy3 streptavidin and Alexa 488 goat anti mouse IgM (1/100 in PBS 0.25% triton) overnight at 4°C. Rings were mounted in Mowiol (Fluka).

The anti α-smooth muscle actin antibody (αSMA, Sigma) was diluted 1/200 in PBS, applied 2 hours at room temperature and revealed using an Alexa 488 goat anti-mouse IgG2a.

TUNEL staining was carried out on chick PAF-fixed CAM sections, using an in situ cell death detection kit with fluorescein (Roche Diagnostics), according to the manufacturer's instructions.

In situ hybridization

In situ hybridization was performed on chick CAM sections, using avian EC-specific c-*ets*1 or *VEGF-R2* antisense riboprobes (Vandenbunder et al., 1989; Eichmann et al., 1993). The protocol, previously described (Eichmann et al., 2000), was followed by QH1 immunostaining revealed by a Texas Red-conjugated anti mouse IgM.

Quantification of QH1$^+$ cells

Observation and counting were performed with Leica or Olympus microscopes. Confocal images were acquired using a Leica TCS SP2 confocal microscope. For each harvested tissue and organ, serial sections were prepared. The number of QH1$^+$ cells in chick tissues was counted manually (×25 objective, final magnification ×110) on a total of 12,000 sections. To calculate the percentage of QH1$^+$ECs integrated in vessels or in the interstitium, one section was randomly chosen from 24 different samples and the number of QH1$^+$ECs integrated in vessels versus all QH1$^+$ECs was determined. The same procedure was applied on 12 different samples to calculate this percentage during mobilization processes.

All cell numbers are expressed as mean±s.e.m. Statistical analysis was carried out using Mann-Whitney's test. $P<0.05$ was considered significant.

RESULTS

Embryonic EPCs survive and differentiate in the circulation

To test whether embryonic EPCs survived in the circulation and differentiated into viable ECs, cell suspensions were prepared from E2 quail paraxial and splanchnopleural mesoderms (Fig. 1A), two tissues known to harbor EPCs (Pardanaud et al., 1996). Cell suspensions were injected into E2 chick host hearts (n=10, Fig. 1A). Histological analysis was carried out using the QH1 monoclonal antibody, which recognizes quail ECs and HCs but does not label quail mural cells (Pardanaud et al., 1987; Etchevers et al., 2001). Serial sections prepared from injected embryos at E3 showed that

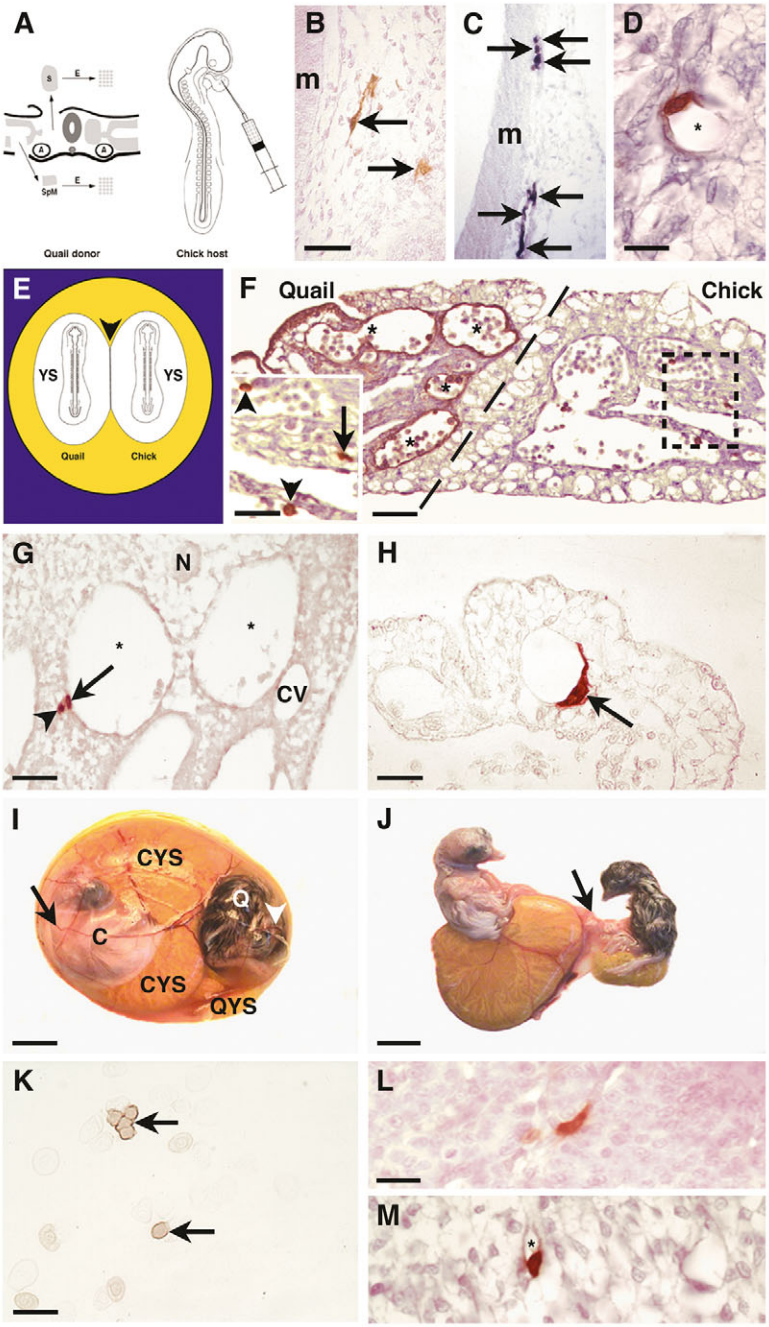

Fig. 1. Survival of embryonic EPCs in the circulation and emergence of CECs. (**A**) Schemes illustrating, on the left, the preparation of E2 quail EPCs from somites (S) and splanchnopleural mesoderm (SpM) after enzymatic digestion (E), on the right, the intracardiac injection of cell suspensions in E2 chick hosts. A, aorta. (**B-D**) Transverse sections of chick embryos that received an intracardiac injection of quail somitic (B,D) or splanchnopleural cells (C). (B,C) Two days after injection, QH1$^+$ECs (arrows) migrate in the mesenchyme close to the mesencephalic epithelium (m). Scale bar: 25 μm. (D) A QH1$^+$EC (brown) is detected in a limb vessel (*) 14 days after the injection. Scale bar: 30 μm. (**E**) Scheme of ex ovo parabiosis (see text for details). YS, yolk sac. (**F**) Transverse section in the region of contact between the two embryos: the broken line delimits the quail territory on the left, with QH1$^+$ vessels (*), and the chick territory on the right, with QH1$^-$ vessels. Scale bar: 70 μm. The inset is a higher magnification of the outlined region: vascular connections are established as QH1$^+$EC (arrow) and HCs (arrowheads) are present in the chick. Scale bar: 35 μm. (**G**) Transverse section in a chick embryo showing a QH1$^+$EC (arrow) and a QH1$^+$HC (arrowhead). CV, cardinal vein; N, notochord; *, aorta. Scale bar: 50 μm. (**H**) Yolk sac section from an E4.5 chick embryo that received an intracardiac injection of E3 quail blood cells: a QH1$^+$EC reaches a vitelline vessel. Scale bar: 30 μm. (I-M) Parabiosis experiments. (**I**) Aspect of an E15 parabiosis in the egg. The chick (C) and quail (Q) embryos, together with their yolk sac (CYS and QYS, respectively), are wrapped into their respective CAM: the arrow indicates a chick CAM vessel; the arrowhead indicates a quail CAM vessel. Scale bar: 15 mm. (**J**) When dissected, the two CAMs appear fused (arrow). Scale bar: 20 mm. (**K**) Blood sample of an E8 chick embryo from a parabiosis: QH1$^+$ cells (arrows) prove the establishment of vascular connections between the embryos. Scale bar: 15 μm. (**L**,**M**) Isolated morphologically distinct QH1$^+$ECs present in a thymus (L) and in a lung capillary (asterisk in M) of E14 chick embryos. Scale bar: 25 μm.

QH1$^+$EC integrated everywhere in the embryo. Owing to the intracardiac injection, a majority of QH1$^+$ECs directly reached the carotids and were found in the perineural mesenchyme surrounding the diencephalon and the mesencephalon (Fig. 1B,C). They also participated to the vascularization of the heart, mesonephros, liver (data not shown) and limb buds, where they were detected up to 14 days after injection (Fig. 1D).

Emergence of CECs/EPCs

To determine if CECs/EPCs circulated in the embryo, we developed an ex ovo parabiosis model (Fig. 1E). E2 quail and chick blastoderms were isolated together with their developing yolk sac and placed on a semi-solid medium in a petri dish. Sectioning of the marginal sinus of each embryo and suturing of the edges facilitated establishment of vascular connections. After 48 hours, histological analysis (n=6, stages 15-19HH) (Hamburger and Hamilton, 1951) showed that the embryos had established vascular anastomoses, as attested by the presence of QH1$^+$HCs and ECs in chick territories (Fig. 1F). Circulating QH1$^+$ECs and HCs invaded virtually all chick tissues, including the yolk sac vessels, the perineural vascular plexus, the heart, the aorta (Fig. 1G) and the splanchnopleural mesoderm. CECs/EPCs were thus present in the circulation at E2 and reached blood vessels, albeit in low numbers.

To confirm the presence of CECs/EPCs in the circulation, blood was harvested from quail embryos at different developmental stages and white cells were injected into E2 chick hearts (Fig. 1A, right panel). Histological analysis between E3 and E16 showed that blood collected from E3 (n=4), E4 (n=11), E5 (n=2) and E15 (n=4) quail embryos contained QH1$^+$CECs/EPCs that participated to the host vascularization, in particular in the head, the visceral organs and the yolk sac (Fig. 1H). As observed with injections of angioblasts, CECs/EPCs survived at least until E16. In all three experimental models, i.e. intracardiac injections of white blood cells or EPC-containing tissues and ex-ovo parabioses, QH1$^+$CECs/EPCs were either integrated into small vessels or present in the interstitium.

CECs/EPCs in classical parabiosis

To follow the behavior of embryonic CECs/EPCs during later stages, we performed chick-quail parabioses. An E2 quail embryo with its yolk was transferred into an E2 chick egg (Fig. 1I). After several days, the two CAMs established contact and developed vascular connections between the embryos. The surviving parabioses (12%) were sacrificed between E7 and E15 (Fig. 1I,J). To verify that vascular connections were established, blood smears from the chick blood were examined for the presence of QH1$^+$ cells (Fig. 1K). Vascular bridges had not yet formed at E7, as attested by the absence of QH1$^+$ cells in the chick blood (0/13). Vascular connections began to form between E8 and E10 (39/70) and were always present after E10 (161/161).

QH1$^+$CECs/EPCs were present in various tissues, irrespective of their embryonic origin: head, limbs, bone marrow, feather buds, dermis, muscles, heart, mesonephros, metanephros, spleen, liver, thymus, lung, gallbladder, gut, pancreas, yolk sac and CAM (Fig. 1L,M and data not shown).

Most QH1$^+$CECs/EPCs were found in the interstitium. In addition to their distinctive elongated morphology, these ECs were characterized by their expression of three EC-specific markers: *Sambucus nigra* lectin (Fig. 2A-C), c-*ets*-1 (not shown) and *VEGFR*-2 (Fig. 2D,E). Elongated QH1$^+$ECs did not express macrophage markers LEP (Fig. 2F-H) or LEA (Fig. 2I-L) while many round QH1$^+$HCs were LEP$^+$ and LEA$^+$ (Fig. 2F-L). Elongated QH1$^+$ECs were also negative for the GRL2 antigen, which labels thrombocytes, myeloid and erythroid progenitors (Thomas et al., 1993) (Fig. 2M-O). By contrast, some round QH1$^+$HCs expressed GRL2 (Fig. 2M-O). Taken together, this labeling showed that ECs could be clearly distinguished from HCs both by morphology and marker expression. As expected, quail HCs of the myeloid and macrophage lineage are present in chick tissues after parabiosis (Fig. 2P). QH1$^+$ Kupffer-like HCs were observed in the liver and granulocytes or osteoclasts in the bone marrow (Fig. 2Q). QH1/αSMA double staining showed that QH1$^+$HCs or CECs/EPCs were not preferentially associated with the vessel wall (Fig. 2R-T).

Counting of the number of QH1$^+$CECs/EPCs integrated in the interstitium of chick tissues showed that their number never exceeded 50 cells/mm^3 in hearts, livers or wings retrieved from E14-15 parabioses (n=22), while this number decreased to 3-6 cells/mm^3 in E8 parabioses (whole embryos, n=2; wings, n=9). Interestingly, in the brain, this number was less than 1 cell/mm^3 (E9, n=3; E14, n=3).

In all chick tissues, a small but significant fraction of QH1$^+$CECs/EPCs integrated into vessels, including capillaries, veins and more rarely lymphatics (33/571=6%, Fig. 3A-F), but never reached major vessels or formed whole tubes. Confocal microscopy of in toto QH1/*Sambucus nigra* lectin double staining on chick CAM showed that QH1$^+$/Sambucus$^+$ ECs could be integrated into the superficial chick vascular plexus as isolated cells (Fig. 3F) and, in few cases, as small groups of cells (not shown). Under the superficial layer, QH1$^+$/Sambucus$^+$ ECs often connected together and formed vascular cords (Fig. 3G-I). These structures did not form a lumen as we never observed consecutive sections of QH1$^+$ endothelia. At the limit of these cords, vascular tips protruded and could contact the endothelial plexus (Fig. 3G,H) or chick QH1$^-$/Sambucus$^+$ cords (Fig. 3I). Sometimes, these cords were found to bridge the chick vasculature (Fig. 3I).

To determine if CECs/EPCs conserved migratory potential after tissue integration, a secondary grafting experiment step was performed using two E15 parabioses. A piece of the chick liver from a parabiosis was retrieved and grafted on an E8 chick host CAM in close contact with either E3 chick limb or visceral buds. In the four cases examined 6 days later, each grafted 'parabiotic' liver contained one QH1$^+$EC (Fig. 3J). In two cases, one QH1$^+$EC migrated to an associated limb (Fig. 3K) and one to a grafted visceral bud (not shown). Furthermore, QH1$^+$ECs reached sinusoids in two host livers (Fig. 3L). Taken together, all the experiments presented here confirmed the existence of a small reservoir of CECs/EPCs in the embryo.

Mobilization of CECs/EPCs

Wounds on the wing

The kinetics of CECs/EPCs mobilization were studied during the wound healing process. An incision in the ulna was performed on a wing of chick embryos from E13 parabioses (Fig. 4A) and the embryos were sacrificed 6-48 hours later. Macroscopic observation showed that the healing process took place rapidly as the wound depth was reduced within 6 hours (Fig. 4B). QH1 staining showed that already at 6 hours, a significantly greater number of QH1$^+$CECs/EPCs invaded the wounded wings compared with the number of QH1$^+$CECs/EPCs in control chick wings (Fig. 5A). The number of QH1$^+$CECs/EPCs remained high up to 48 hours after wounding, corresponding to E15, the last day before the quail hatched (Fig. 5A). The invading QH1$^+$CECs/EPCs were distributed uniformly throughout the wounded wing, even in areas distant from the wound site. Most of the QH1$^+$ECs were isolated and located in

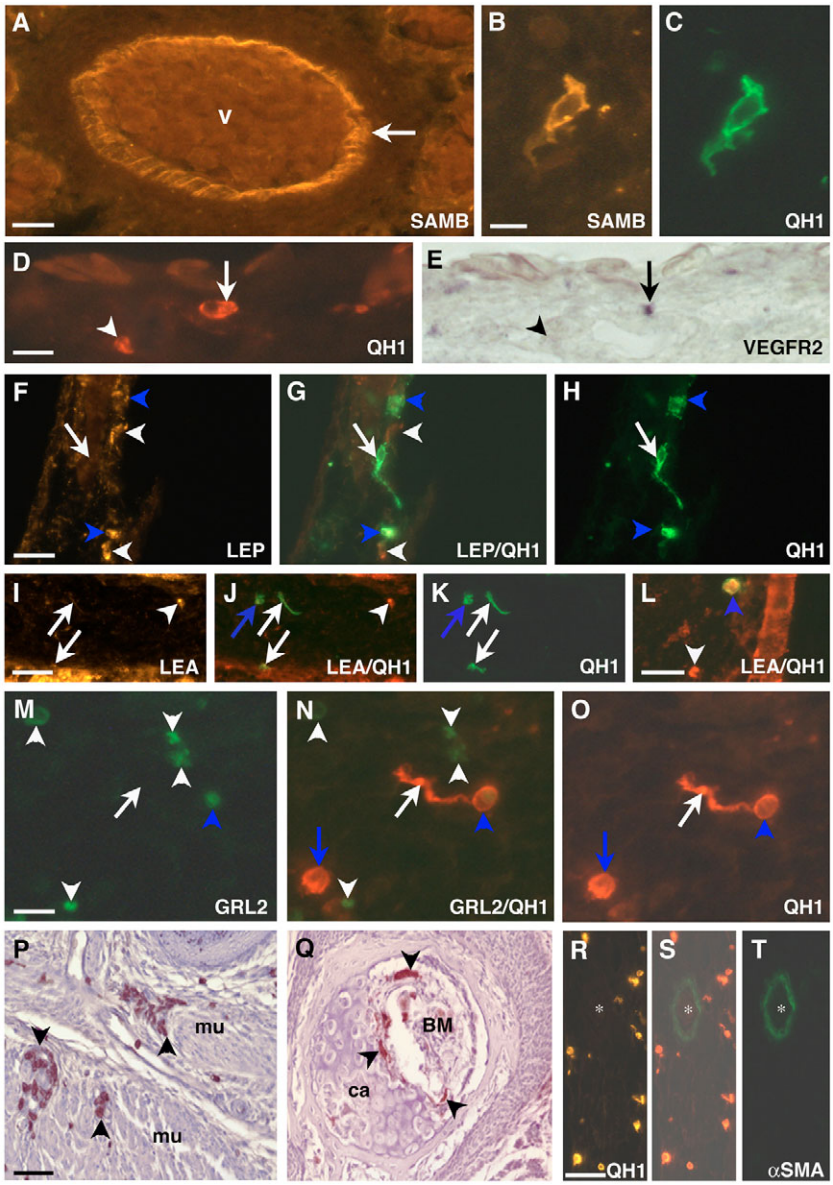

Fig. 2. Identification of quail ECs and HCs in chick CAM after parabiosis. (**A-C**) *Sambucus nigra* lectin (SAMB)/QH1 double staining. (A) The endothelium (arrow) of a chick vessel (v) stained by SAMB. Scale bar: 25 μm. (B,C) One isolated interstitial quail SAMB$^+$/QH1$^+$EC. Scale bar: 15 μm. (**D**,**E**) QH1/VEGFR2 double staining: a QH1$^+$EC expresses VEGFR2 transcripts (arrow); a QH1$^+$HC does not (arrowhead). Scale bar: 25 μm. (**F-H**) LEP/QH1 double staining: an elongated LEP$^-$/QH1$^+$EC (white arrow) surrounded by chick (LEP$^+$/QH1$^-$, white arrowheads) and quail (LEP$^+$/QH1$^+$, blue arrowheads) macrophages. Scale bar: 25 μm. (**I-L**) LEA/QH1 double staining: (I-K) two quail LEA$^-$/QH1$^+$ECs (white arrows) present in the vicinity of a chick LEA$^+$/QH1$^-$ macrophage (white arrowhead) and a round quail LEA$^-$/QH1$^+$HC (blue arrow). Scale bar: 25 μm. (L) One quail (LEA$^+$/QH1$^+$, blue arrowhead) and one chick (LEA$^+$/QH1$^-$, white arrowhead) macrophage are present. Scale bar: 15 μm. (**M-O**) GRL2/QH1 double staining: an elongated GRL2$^-$/QH1$^+$EC (white arrow) identified among chick (GRL2$^+$/QH1$^-$, white arrowheads) and quail (GRL2$^+$/QH1$^+$, blue arrowhead) hematopoietic precursors, and a quail GRL2$^-$/QH1$^+$ macrophage (blue arrow). Scale bar: 10 μm. (**P-T**) QH1$^+$HC distribution. QH1$^+$HCs are found in muscle as extravasated cells (P, arrowheads) or in the bone marrow as osteoclasts (Q, arrowheads). Scale bar: 80 μm. BM, bone marrow; ca, cartilage; mu, muscle. (R-T) QH1/αSMA double staining shows that QH1$^+$HCs never reach vessel walls. *, vessel lumen. Scale bar: 70 μm.

the interstitium of the dermis, the perichondrium, the muscles, the feather buds and, in a few cases, the bone marrow (Fig. 4C). Their integration in host endothelia remained rare and restricted to small vessels (36/774=5%). In all cases, the mobilization of CECs/EPCs was restricted to wounded wings, as the number of QH1$^+$ECs invading the contralateral wings (Fig. 4D) or other organs, such as the heart and the liver, was not altered (Fig. 5A). The total number of QH1$^+$HCs in wounded wings varied greatly between experiments but no significant difference between control, contralateral and wounded limbs was found (Fig. 5B). However, the proportion of extravasated QH1$^+$HCs appeared higher in the operated wings than in the controls, in particular in the vicinity of the wound (Fig. 4C,D). Thus, it seemed that wounding stimulated mobilization of circulating QH1$^+$ cells.

Wounds on CAM

Wounds were made on the chick CAM from E10 parabioses. In a restricted CAM area circumscribed by a silicone ring, either small arteries or veins were cut. One day later, the wounds on veins lead to an invasion of QH1$^+$CECs/EPCs, which were again mainly found in an interstitial location (Fig. 4E). Their number was significantly increased compared with the number of QH1$^+$CECs/EPCs found in control CAMs (Fig. 5C). Surprisingly, wounding of arteries did not stimulate invasion of QH1$^+$CECs/EPCs (Fig. 4F, Fig. 5C,). Despite a great variability, the total number of invading QH1$^+$HCs was generally lower after wounding of arteries compared with veins. As observed after wounding of wings, the number of extravasated QH1$^+$HCs increased after wounding of veins (Fig. 4E,F), suggestive of increased mobilization of circulating cells. To determine survival of QH1$^+$ cells in the host CAM, a QH1/TUNEL double staining was performed and showed that QH1$^+$CEC/EPC and HC nuclei were never apoptotic (Fig. 4G,H).

Grafts of organ rudiments

To test whether CECs/EPCs were mobilized during angiogenesis and vasculogenesis processes, E3 chick limb buds (n=11) or visceral organs (n=4) were grafted on the chick CAM in E10 parabioses. After 1 to 9 days (Fig. 4I,J), while numerous QH1$^-$ chick vessels vascularized the grafts, a great contingent of quail QH1$^+$CECs/EPCs

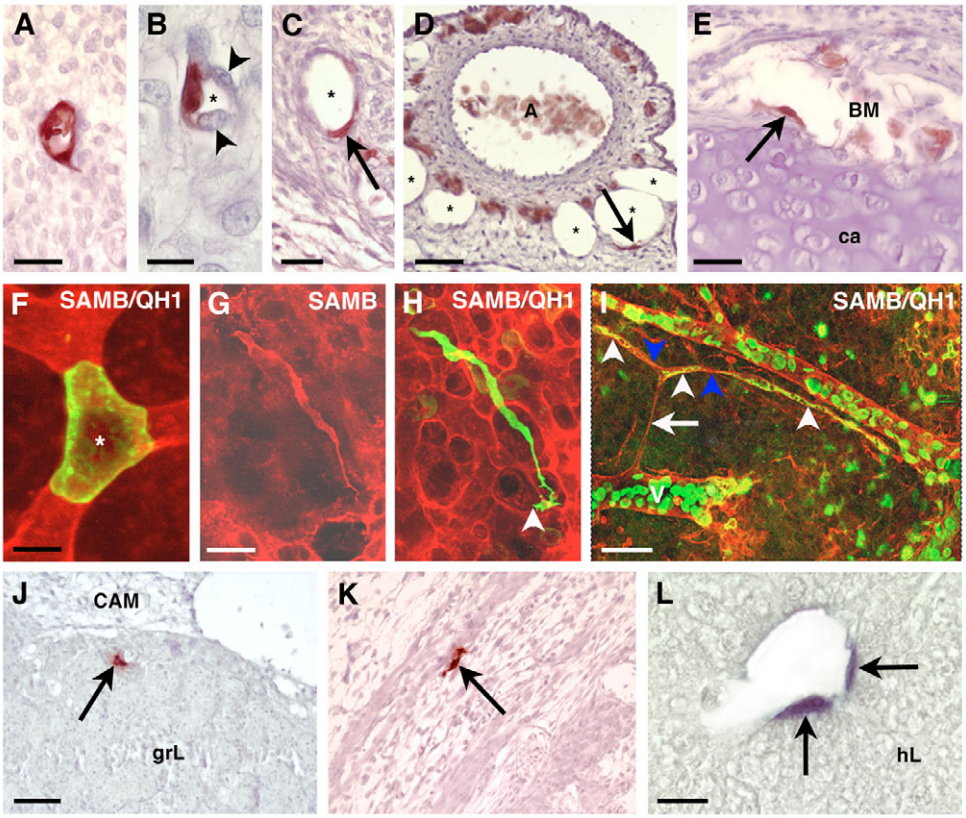

Fig. 3. Behavior of CECs/EPCs. (A-I) QH1$^+$EC distribution. (**A**) A whole section of a capillary is quail-derived. Scale bar: 50 μm. (**B**) Chimeric capillary (*) with a QH1$^+$EC (brown) and two chick QH1$^-$ECs (arrowheads). Scale bar: 20 μm. (**C**) A larger vein (*) with one QH1$^+$EC (arrow). Scale bar: 45 μm. (**D**) Among lymphatic vessels (*) surrounding a CAM artery (A), one is chimeric (arrow). Scale bar: 90 μm. (**E**) A QH1$^+$EC (arrow) in the bone marrow. Scale bar: 45 μm. (F-I) Confocal images of whole-mount SAMB/QH1 double staining on chick CAM. (**F**) A quail SAMB$^+$/QH1$^+$EC (*) integrated in the superficial chick SAMB$^+$/QH1$^-$ vascular plexus. Scale bar: 10 μm. (**G**,**H**) A SAMB$^+$/QH1$^+$ vascular cord in contact with the chick SAMB$^+$ plexus (arrowhead). Scale bar: 15 μm. (**I**) A chimeric vascular cord with quail (white arrowheads) and chick (blue arrowheads) regions linked to a chick vessel (V) through a chick vascular bridge (arrow). Scale bar: 40 μm. (J-L) Conserved migratory potential of CECs/EPCs after tissue integration. (**J**) Chick 'parabiotic' liver (grL) grafted onto the CAM of a chick host: one QH1$^+$EC (arrow) is present. (**K**) A QH1$^+$EC (arrow) is present in the mesenchyme of an E3 chick limb bud grafted next to a chick 'parabiotic' liver. Scale bar: 80 μm. (L) Two QH1$^+$ECs (arrows) originating from the grafted 'parabiotic' liver have reached a sinusoid of the chick host liver (hL). Scale bar: 15 μm.

migrated into the rudiments (Fig. 4K,L). Most of these cells were isolated and migrated interstitially. Besides QH1$^+$ECs, QH1$^+$HCs also invaded the tissues. Four days after grafting, we noted that the number of QH1$^+$CECs/EPCs was higher in the limb buds than in the visceral organs (Fig. 5D).

To determine if the increase in the number of quail CECs/EPCs was due to increased mobilization or proliferation, BrdU incorporation was performed. In a limb bud grafted for 9 days on the CAM, many BrdU$^+$ nuclei were detected in the dermis, the perichondrium and the feather buds (Fig. 4M). The incorporation was also high in the host heart (Fig. 4N). However, the mitotic index of invasive QH1$^+$CECs/EPCs, calculated by counting the number of QH1$^+$/BrdU$^+$ECs (Fig. 4O) versus all QH1$^+$ECs was low (7%, 7/105, Fig. 4M). This index was equivalent to the index obtained for QH1$^+$CECs/EPCs in the host chick heart (8%, 23/272, Fig. 4N). Thus, this result suggested that the increase in QH1$^+$CEC/EPC number was not related to proliferation but to increased mobilization.

Grafts of endothelin 1-producing cells

Suspensions of endothelin 1-producing CHO cells, known to stimulate angiogenesis (Cruz et al., 2001), or control cells were deposited on the chick CAM from E9 parabioses. The eggs were sacrificed after 1-5 days. Although control cells never survived in these conditions (n=3), transfected cells gave rise to well developed nodules at the surface and inside the CAM (n=7, Fig. 6A,B). These nodules were vascularized by chick vessels in which QH1$^+$CECs/EPCs could be integrated (Fig. 6B,C). However, the majority of QH1$^+$CECs/EPCs were interstitially located (Fig. 6B,C).

VEGF-induced angiogenesis

VEGF application on chick CAM from E10 parabioses induced a sprouting angiogenic response (Fig. 6D,E) quantified by a higher number of vessel branches (Fig. 5E). Histological analysis showed significant inflammation leading to the invasion of numerous QH1$^+$HCs in the CAM (Fig. 6F,G). QH1$^+$CECs/EPCs were present in the interstitium and the capillary endothelium of the treated areas. Their number did not vary significantly between VEGF-treated and PBS-treated CAMs (Fig. 5F, Fig. 6F,G). The vascular density being different in these two groups, as determined by the increase in vessel branching after VEGF treatment (Fig. 6F,G), we calculated the number of quail QH1$^+$CECs/EPCs per branch. Despite a certain variability between cases, this ratio was not statistically different in PBS-

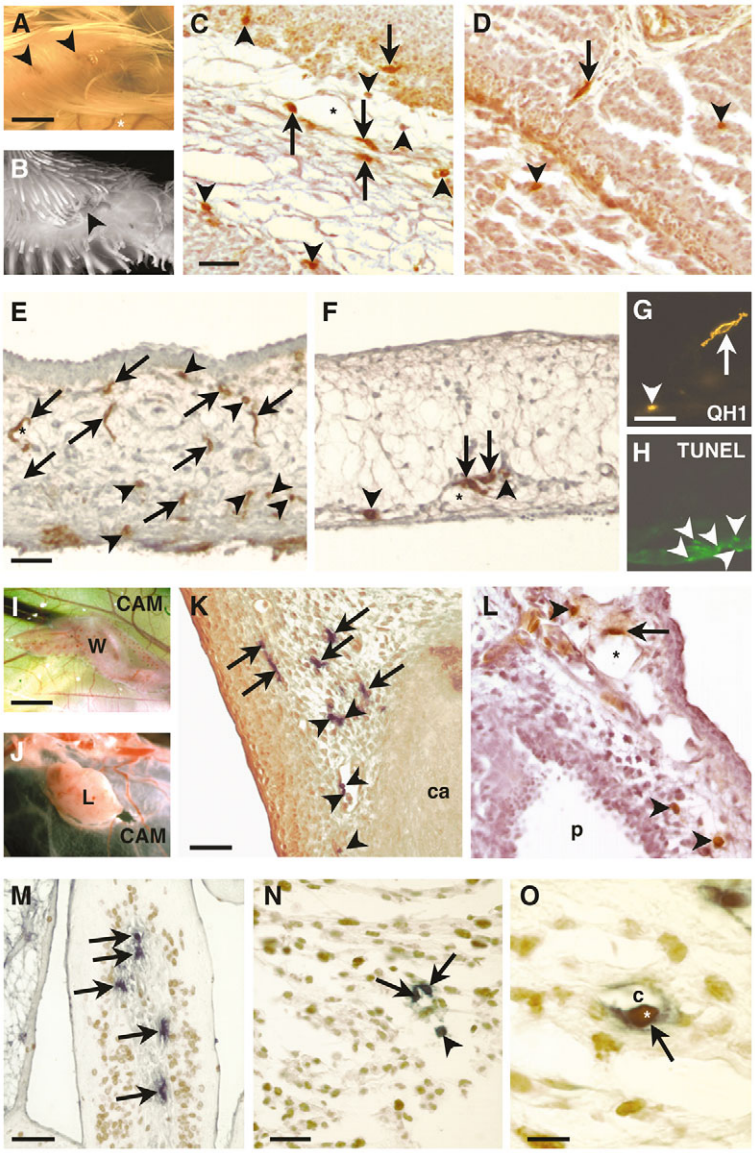

Fig. 4. Mobilization of CECs/EPCs in parabiosis (part 1). (**A**) An E13 chick wing immediately after a wound: the limb is on the CAM (*) and the size of the wound is delimited by two hemorrhagic dots (arrowheads). (**B**) The wound (arrowhead) 1 day later, after the shortening of feather buds. Scale bar: 5 mm. (**C**) Transverse section of an E14 wounded wing showing elongated QH1$^+$ECs (arrows) in the interstitium and integrated in a vessel (*) as well as round QH1$^+$ HCs (arrowheads). In a contralateral E14 wing (**D**), QH1$^+$ECs (arrow) and QH1$^+$HCs (arrowheads) are less numerous. Scale bar: 100 μm. (**E**,**F**) Sections of chick CAM from parabiosis 1 day after wounding. (E) After wounding of veins, there are numerous QH1$^+$ECs (arrows) and QH1$^+$HCs (arrowheads). (F) After wounding of arteries, QH1$^+$ECs (arrows) and HCs (arrowheads) are more rare; *, vessel. Scale bar: 40 μm. (**G**,**H**) QH1/TUNEL double staining illustrating that QH1$^+$CECs/EPCs (arrow in G) and QH1$^+$HCs (arrowhead in G) are TUNEL$^-$, while apoptotic nuclei are present in the CAM ectoderm (arrowheads in H). Scale bar: 35 μm. (**I**) Chick wing (W) 6 days after grafting onto the CAM of a 'parabiotic' chick embryo. (**J**) Chick lung (L) 9 days after grafting onto the CAM of a 'parabiotic' chick embryo. Scale bar: 3 mm. (**K**) Transverse section of a grafted limb showing QH1$^+$ECs (arrows) and QH1$^+$HCs (arrowheads) around the cartilage (ca). (**L**) transverse section of a grafted lung with a QH1$^+$EC (arrow) integrated in a vessel endothelium (*) and QH1$^+$HCs (arrowheads) in the mesenchyme surrounding a parabronchius (p). Scale bar: 100 μm. (**M-O**) BrdU incorporation in an E15 parabiosis 9 days after grafting of a chick limb bud onto the chick CAM. (M) In a feather bud of the grafted limb, numerous nuclei are BrdU$^+$ (brown dots); however, QH1$^+$ECs (arrows) present in the pulp are BrdU$^-$. Scale bar: 70 μm. (N) In the corresponding 'parabiotic' host chick heart, BrdU is incorporated into the myocardium (brown dots), but QH1$^+$ECs (arrows) and QH1$^+$HCs (arrowhead) are BrdU$^-$. Scale bar: 35 μm. (O) A double stained QH1$^+$/BrdU$^+$EC in a myocardiac capillary (c), the brown nucleus (*) is surrounded by the dark blue QH1 staining. Scale bar: 15 μm.

treated and VEGF-treated CAMs (Fig. 5G). Thus, VEGF-induced sprouting angiogenesis on the CAM did not mobilize QH1$^+$CECs/EPCs.

Mobilization of CECs/EPCs occurs prior to bone marrow formation

We studied the mobilization of CECs/EPCs before the bone marrow differentiated. In the first set of experiments, the chick wing of E8 parabioses was wounded (n=9). In the second set of experiments, a chick limb bud was grafted on the chick CAM of E6.5 parabioses (n=11). In both cases, the QH1 analysis was carried out at E9, a developmental stage when the quail bone marrow had not yet differentiated.

During the wound healing process, QH1$^+$CECs/EPCs invaded the wounded wings (Fig. 6H). Their number was significantly increased compared with the number of QH1$^+$CECs/EPCs that colonized control or contralateral wings (Fig. 7). Compared with wounding of wings of parabioses at E13, the number of invading CECs/EPCs was reduced. However, owing to technical constraints, both the site and the size of the wound were different, so these results are difficult to compare directly. QH1$^+$HCs were also present in these tissues (Fig. 6H) but their number varied greatly and was not significantly different between the experimental groups (not shown).

Circulating QH1$^+$CECs/EPCs also homed to grafted limb buds very efficiently (Fig. 6I). Their number reached 68±54 cells/mm^3, a value that was significantly higher when compared with the number of QH1$^+$CECs/EPCs in control E8-9 parabiosis wings (6±4 cells/mm^3, P<0.002).

We conclude that the differentiation of the bone marrow is not essential to mobilize CECs/EPCs.

DISCUSSION

Using the quail-chick parabiosis model, we here demonstrate the early emergence and the mobilization of CECs/EPCs in the embryo. The hypothesis that embryonic ECs traveled through the blood stream was previously postulated in the quail-chick chimera system. The quail allantoic bud, grafted in a chick coelom, produced QH1$^+$ECs that colonized the chick tissues, including the bone marrow. Owing to the distance between the initial location of these cells, the coelom, and their final location, the bone marrow, the migration of QH1$^+$ECs was likely to occur through the circulation (Caprioli et al., 1998).

We first verified that avian EPCs survived and differentiated in the circulation as recently shown for murine ECs (Yamashita et al., 2000), then chose the quail-chick parabiosis model to experimentally demonstrate the existence of CECs/EPCs. Previous studies using quail-chick parabioses between E6 and E10 never detected QH1$^+$ECs in the chick embryo (Kurz and Christ, 1998; Kurz et al., 2001). The absence of QH1$^+$ECs in those tissues was probably related to our observation that vascular connections between quail and chick CAM were not systematically established prior to E10 and that the participation of QH1$^+$CECs/EPCs to chick vasculature between E7 and E10 was very low.

Recent studies showed that ex vivo expanded embryonic EPCs were recruited during adult tumorigenesis (Vajkoczy et al., 2003; Yurugi-Kobayashi et al., 2003). When fluorescent E7.5 mouse EPCs were introduced in the circulation of rat C6 glioma tumor-bearing nude mice, they were specifically arrested within the tumor vasculature, extravasated into the interstitium and sometimes incorporated into functional capillaries (Vajkoczy et al., 2003). Unlike our observations, mouse EPCs never participated to the host vasculature in normal organs. This could be due to: (1) the method of analysis using intravital fluorescence videomicroscopy, which only allowed superficial measures while our histological analysis screened the organ vasculature and detected rare QH1$^+$ECs; and/or (2) the adult mouse model, in which organogenesis was completed and the vascular system was quiescent, while our experiments concerned growing embryos in which organogenesis and endothelial growth were actively ongoing.

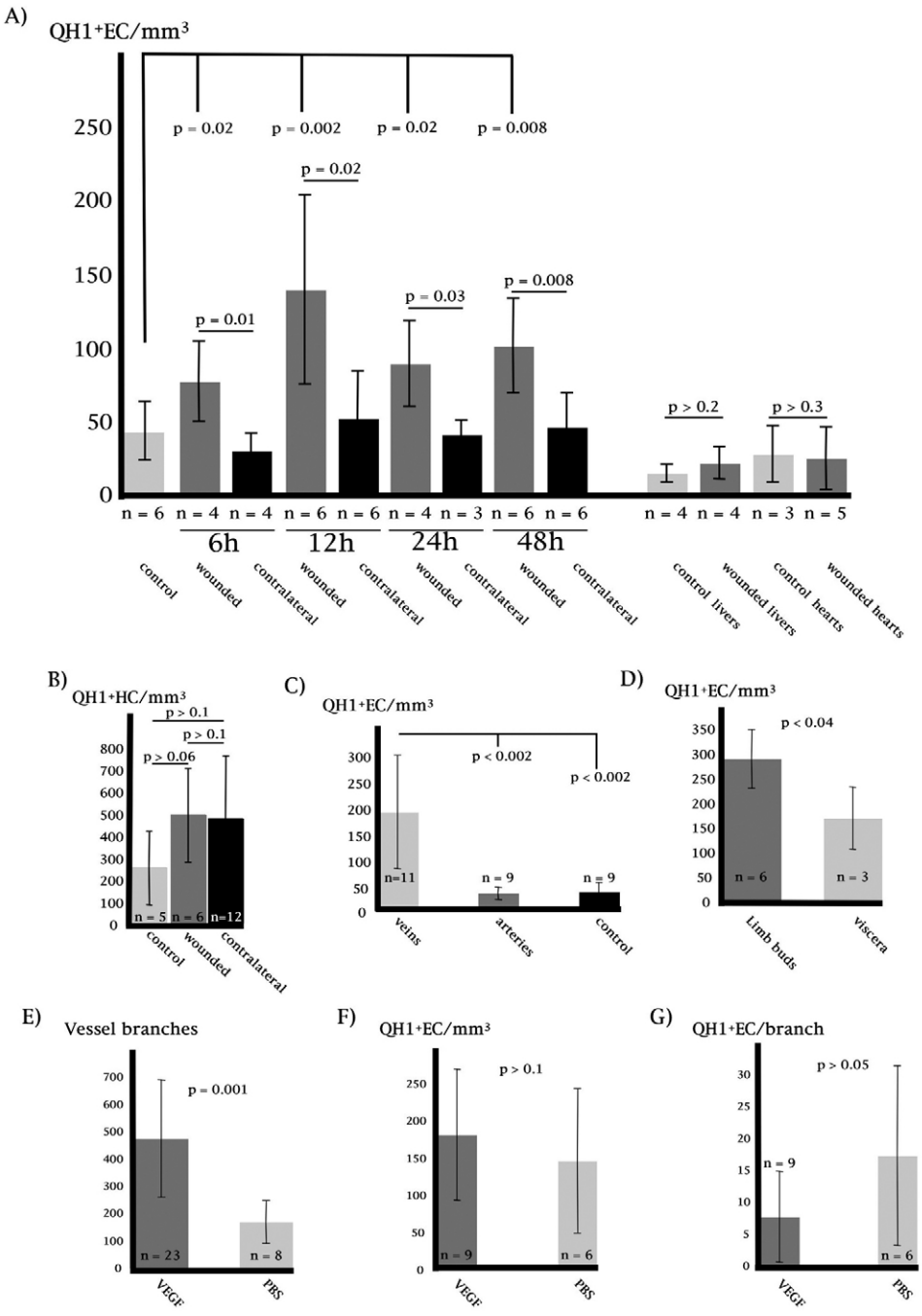

Fig. 5. Quantification of the QH1+ cell mobilization. (**A**) Kinetics of the wound healing process: a specific, rapid and significant increase in the number of QH1$^+$ECs in wounded wings in comparison with control limbs or with contralateral wings is observed. The specificity of this mobilization is attested by the similar number of QH1$^+$ECs found in livers and hearts isolated from control or wounded chick embryos. (**B**) During the wound healing process, the QH1$^+$HC number did not vary significantly between control, contralateral and wounded wings. (**C**) Wounds on CAMs lead to a significant increase in the QH1$^+$EC number when veins are injured compared with control CAM or wounded arteries. (**D**) In grafting experiments on CAM, the QH1$^+$EC number is significantly greater in the grafted limb buds than in the viscera. (**E-G**) VEGF-treated CAM assays: while the number of vessel branches is significantly increased in VEGF-treated CAMs (E), by comparison with PBS-treated CAMs (E), the overall QH1$^+$EC number (F) and the number of QH1$^+$ECs per branch (G) do not vary significantly between treated and control CAMs.

Embryonic EPCs invading the tumor did not divide very much after their tissue integration (Vajkoczy et al., 2003). The low mitotic index of CECs/EPCs we obtained agreed with this finding and might explain why the majority of migrating QH1$^+$ECs were alone and never formed a clone. An equivalent low mitotic index is also observed in normal E6-7 chick aortic ECs (Seifert et al., 1992).

Concerning the behavior of EPCs, recent studies showed that invading cells participate to functional blood vessels (Asahara et al., 1999; Vajkoczy et al., 2003; Yurugi-Kobayashi et al., 2003; Tepper et al., 2005). In our parabiosis experiments, QH1$^+$CECs/EPCs could be distinguished from QH1$^+$ circulating HCs by their distinctive elongated morphology and their expression of various EC, but not HC, markers. Of note, we have not observed incorporation of CECs/EPCs or circulating HCs in the vascular wall in any of the experiments performed. However, as QH1 does not recognize pericytes, we cannot exclude the existence of quail-derived circulating pericytes progenitors or transdifferentiation of circulating cells.

In all experimental conditions, a small proportion of CECs/EPCs (5%) integrated into host vessels. Different vessel types were colonized, including capillaries, veins and, more rarely, lymphatics. Larger vessels, especially arteries, were colonized only during early stages of development. Within small vessels, incorporation of CECs/EPCs appeared random, i.e. while some CECs/EPCs were located at vessel branch points (Fig. 3F), others were located in straight vessel segments (Fig. 3A-E). Interestingly, CEC/EPC incorporation did not occur in processes of sprouting angiogenesis such as brain vascularization. The chick brain is vascularized by angiogenic sprouting from the perineural vascular plexus in which CECs/EPCs are integrated. In spite of their presence in this plexus, the number of CECs/EPCs found in the brain of parabiotic chicks was lower than in any other tissue. In VEGF-induced sprouting angiogenesis in the parabiotic CAM, again no significant participation of CECs/EPCs was observed. Taken together, these results suggest that CECs/EPCs adhere and extravasate to host vessels at sites of favorable flow conditions.

Interestingly, in all experimental conditions, most CECs/EPCs were found in an interstitial location. Confocal microscopy showed that these cells exhibited characteristic EC morphology and expressed the EC marker *Sambucus nigra*. Interstitial ECs did not form lumens but remained as cords that contact and bridge the host vasculature. Their function is currently not entirely clear. Although they do not appear to undergo apoptosis, they do not seem to evolve

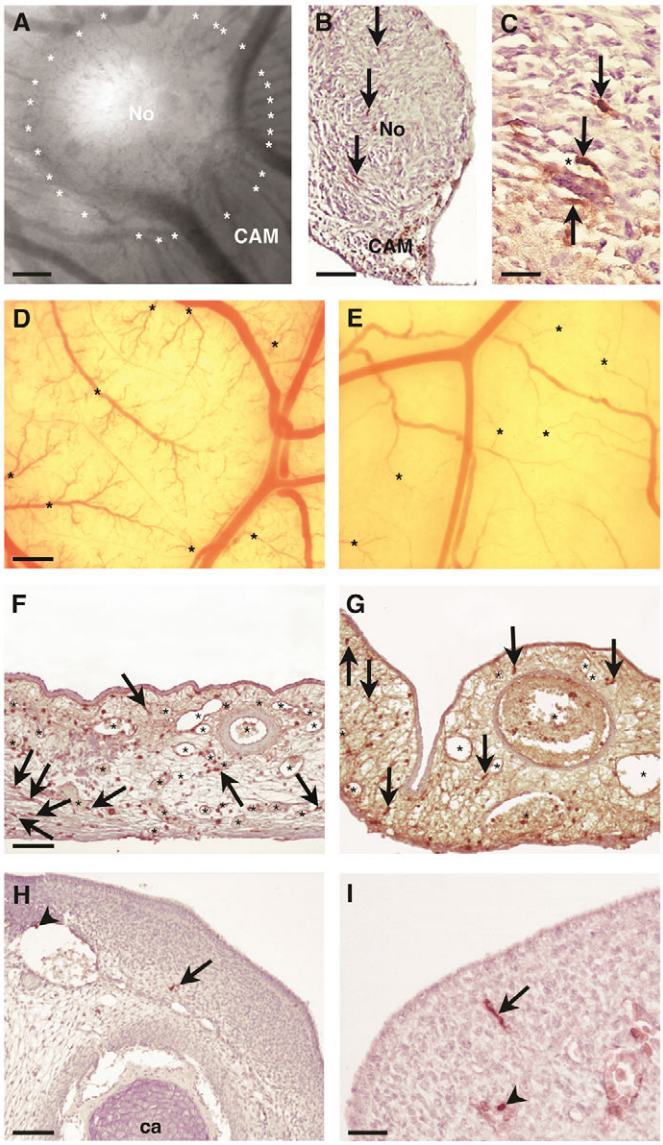

Fig. 6. Mobilization of CECs/EPCs in parabiosis (part 2). (**A**) An endothelin 1-producing CHO nodule (No), 5 days after cellular implantation onto a 'parabiotic' chick CAM. Capillaries are organized in a spoke-wheel formation (*) converging to the nodule. Scale bar: 1 mm. (**B**) The nodule (No) is wrapped in the CAM, and QH1$^+$ECs (arrows) participate in its vascularization. Scale bar: 160 μm. (**C**) Higher magnification of QH1$^+$ECs invading the nodule (arrows): one cell is in a capillary endothelium (*), two are located interstitially. Scale bar: 20 μm. (**D-G**) 'Parabiotic' chick CAM 4 days after VEGF (D) or PBS (E) treatment: increased vessel branching (*) is apparent in D compared with E. Scale bar: 1.5 mm. (F,G) The vessel density (*) is higher in VEGF-treated (F) than in PBS-treated (G) CAM. Although the inflammatory response leads to an invasion of a great number of QH1$^+$HCs (brown dots) in both treatments, the number of QH1$^+$ECs (arrows) is similar. Scale bar: 90 μm. (**H**,**I**) Mobilization in absence of bone marrow: wounds on 'parabiotic' chick wings (H) and grafts of chick limb buds onto 'parabiotic' chick CAM (I) lead to an invasion of QH1$^+$ECs (arrows) and QH1$^+$HCs (arrowheads). ca, cartilage. Scale bars: 90 μm in H; 70 μm in I.

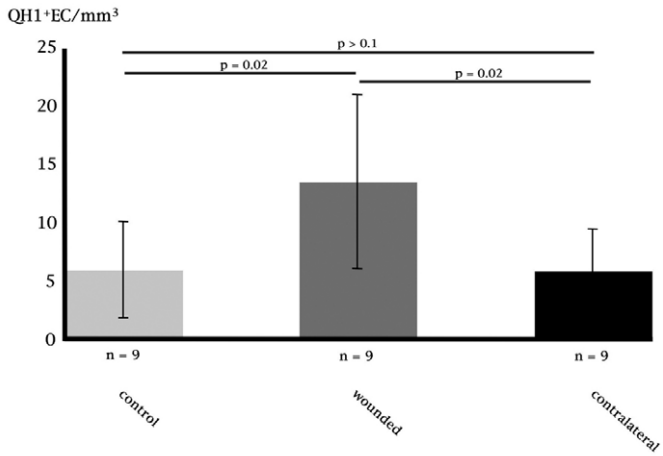

Fig. 7. Mobilization in the absence of bone marrow. The wound healing process results in the mobilization of significantly more QH1$^+$ECs in injured wings compared with control or contralateral limbs.

into functional tubes either, although we have not been able to follow this over a period of more than 48 hours, owing to constraints of the experimental system. It is possible that these cells serve a structural bridging role or alternatively that they secrete paracrine growth factors. In adult ischemic tissues, Urbich and Dimmeler (Urbich and Dimmeler, 2004a) reported that interstitially located EPCs could influence neovascularization in a paracrine manner by releasing pro-angiogenic factors.

Although the number of CECs/EPCs integrated in normal developing tissues was always low, CECs/EPCs were rapidly mobilized during wound healing after an incision in a chick wing. The recruitment of circulating cells to sites of wound healing was also shown in the adult (Asahara et al., 1999; Sivan-Loukiavona et al., 2003; Galiano et al., 2004; Montesinos et al., 2004; Tepper et al., 2005). As in the embryo, adult CECs/EPCs migrated interstitially in the wounded tissue or reached small endothelia but never formed complete tubes (Asahara et al., 1999). In our model, the number of mobilized CECs/EPCs was at least doubled in wounded wings by comparison with control or contralateral limbs. In the adult, a similar ratio was found (Montesinos et al., 2004). Furthermore, the increase in number of QH1$^+$CECs/EPCs already occurred after 6 hours and remained stable until 48 hours, suggesting a rapid mobilization during the establishment of an initial vascular supply to the wounded ischemic tissue.

Wounds on the CAM surprisingly showed that CEC/EPC mobilization was effective only when veins were injured. This result could be related to a mechanical effect involving a rapid vasoconstriction on arteries following injury. This vasoconstriction limited the ischemia around wounds and the CEC/EPC mobilization did not occur. This result could also imply that arteries and veins would have different properties regarding the capacity to respond to an injury and to mobilize CECs/EPCs. This difference might be an additional way to identify the nature of invasive vessels in tumors. The quail-chick parabioses could be an interesting model to study this point by grafting tumors on chick CAM.

The significant difference between QH1$^+$ECs invading the grafted limb buds and the visceral organs was probably linked to the vascularization process operating in these tissues (Pardanaud et al., 1989; Pudliszewski and Pardanaud, 2005). The limb territory, which is vascularized through angiogenesis, was more permissive to the invasion of QH1$^+$CECs/EPCs than were the visceral buds, which are vascularized through vasculogenesis. This invasion could represent an early vascular mobilization that permitted to the grafted ischemic tissues to establish the first vascular connections with the host CAM vessels and avoid necrosis.

As mentioned above, the VEGF-induced sprouting angiogenesis on the CAM did not mobilize CECs/EPCs. Although this result seemed unexpected, VEGF did not always mobilize adult EPCs either (De Palma et al., 2003; Ruzinova et al., 2003). VEGF-stimulated EPCs did not systematically increase the formation of vessels (Young et al., 2002) but seemed to act indirectly on angiogenesis via the recruitment of bone marrow-derived circulating cells (Grunewald et al., 2006; Zentilin et al., 2006). In our model, CECs/EPCs appeared to be principally involved during angiogenic responses related to ischemia and not requiring sprouting, at least during the initial response phase.

We also showed here that CECs/EPCs do not originate from the bone marrow as they were present at stages when this organ was not yet developed. Furthermore, the mobilization of CECs/EPCs was not dependent on this organ as it was effective while the marrow was not differentiated. These observations agreed with recent findings that concluded that the bone marrow was not the source of EPCs (Beck et al., 2003; Gothert et al., 2004; Hillebrands et al., 2002; Machein et al., 2003; Voswinckel et al., 2003) but rather appeared as a niche containing vascular wall progenitors and HCs directly mobilized during neoangiogenesis process (Rajantie et al., 2004; Grunewald et al., 2006). The bone marrow could also provide a useful environment for the multiplication of EPCs because, in our work, their number was more important at stages when this hematopoietic organ had developed.

The original model of E2 parabiosis demonstrated that CECs/EPCs were present early in ontogenesis. To map precisely the origin of CECs/EPCs, quail-chick yolk sac chimeras are currently being generated. In previous studies using E1 yolk sac chimeras, associating a chick blastoderm with a quail yolk sac, scarce QH1$^+$ECs could be found in E2.5-E4 chick embryos, mainly in the cephalic region (Cuadros et al., 1992). These results indicate a yolk sac origin of CECs/EPCs also recently suggested by La Rue et al. (La Rue et al., 2003) using a retroviral labeling strategy.

The lack of lineage-specific markers in the avian model did not permit to distinguish whether QH1$^+$ CECs correspond to progenitors cells or to 'mature' ECs, but owing to their great ability to reach sites of angiogenesis, we favor the hypothesis of EPCs. It has been recently shown that mature CEC were more sticky and remained sequestered within the microvasculature of organs, while undifferentiated cells gained access to tumor microvasculature (Vajkoczy et al., 2003).

In conclusion, we show that embryonic CECs/EPCs are already present early in development and are mobilized during angiogenic processes even in the absence of the bone marrow. The next step will be to determine the factors that regulate mobilization and homing of these cells. It would be also interesting to know how physiopathological conditions such as hypoxia or diabetes modulate the emergence and the role of CECs/EPCs: a recent model of diabetic chicken (Larger et al., 2004) could be used in our parabiosis model.

We thank N. Lamandé for providing us the CHO cells, C. Bréant for the in situ preparations, E. Etienne for assistance with the confocal microscope, and P. Corvol and S. Suchting for the critical reading of the manuscript. This work was supported by Inserm Avenir.

References

Asahara, T., Murohara, T., Sullivan, A., Silver, M., Van der Zee, R., Li, T., Witzenbichler, B., Schattemen, G. and Isner, J. M. (1997). Isolation of putative progenitor endothelial cells for angiogenesis. *Science* **275**, 964-967.

Asahara, T., Masuda, H., Takahashi, T., Kalka, C., Pastore, C., Silver, M., Kearne, M., Magner, M. and Isner, J. M. (1999). Bone marrow origin of endothelial progenitor cells responsible for postnatal vasculogenesis in physiological and pathological neovascularization. *Circ. Res.* **85**, 221-228.

Beck, H., Voswinckel, R., Wagner, S., Ziegelhoeffer, T., Heil, M., Helisch, A., Schaper, W., Acker, T., Hatzopoulos, A. K. and Plate, K. H. (2003). Participation of bone marrow-derived cells in long-term repair processes after experimental stroke. *J. Cereb. Blood Flow Metab.* **23**, 709-717.

Brooks, P. C., Montgomery, A. M. and Cheresh, D. A. (1999). Use of the 10-day-old chick embryo model for studying angiogenesis. *Methods Mol. Biol.* **129**, 257-269.

Caprioli, A., Jaffredo, T., Gautier, R., Dubourg, C. and Dieterlen-Lièvre, F. (1998). Blood-borne seeding by hematopoietic and endothelial precursors from the allantois. *Proc. Natl. Acad. Sci. USA* **95**, 1641-1646.

Carmeliet, P. (2003). Angiogenesis in health and disease. *Nat. Med.* **9**, 653-660.

Cherqui, S., Kurian, S. M., Schussler, O., Hewel, J. A., Yates, J. R., III and Salomon, D. R. (2006). Isolation and angiogenesis by endothelial progenitors in the fetal liver. *Stem Cells* **24**, 44-54.

Cogle, C. R. and Scott, E. W. (2004). The hemangioblast: cradle to clinic. *Exp. Hematol.* **32**, 885-890.

Cruz, A., Parnot, C., Ribatti, D., Corvol, P. and Gasc, J. M. (2001). Endothelin-1, a regulator of angiogenesis in the chick chorioallantoic membrane. *J. Vasc. Res.* **38**, 536-545.

Cuadros, M. A., Coltey, P., Carmen Nieto, M. and Martin, C. (1992). Demonstration of a phagocytic cell system belonging to the hemopoietic lineage and originating from the yolk sac in the early avian embryo. *Development* **115**, 157-168.

De Palma, M., Venneri, M. A., Roca, C. and Naldini, L. (2003). Targeting exogenous genes to tumor angiogenesis by transplantation of genetically modified hematopoietic stem cells. *Nat. Med.* **9**, 789-795.
Eichmann, A., Marcelle, C., Bréant, C. and Le Douarin, N. M. (1993). Two molecules related to the VEGF receptor are expressed in early endothelial cells during avian embryonic development. *Mech. Dev.* **42**, 33-48.
Eichmann, A., Yuan, L., Bréant, C., Alitalo, K. and Koskinen, P. J. (2000). Developmental expression of pim kinases suggests functions also outside of the hematopoietic system. *Oncogene* **19**, 1215-1224.
Etchevers, H. C., Vincent, C., Le Douarin, N. M. and Couly, G. F. (2001). The cephalic neural crest provides pericytes and smooth muscle cells to all blood vessels of the face and forebrain. *Development* **128**, 1059-1068.
Galiano, R. D., Tepper, O. M., Pelo, C. R., Bhatt, K. A., Callaghan, M., Bastidas, N., Bunting, S., Steinmetz, H. G. and Gurtner, G. C. (2004). Topical vascular endothelial growth factor accelerates diabetic wound healing through increased angiogenesis and by mobilizing and recruiting bone marrow-derived cells. *Am. J. Pathol.* **164**, 1935-1947.
Gehling, U. M., Ergun, S., Schumacher, U., Wagener, C., Pantel, K., Otte, M., Schuch, G., Schafhausen, P., Mende, T., Kilic, N. et al. (2000). In vitro differentiation of endothelial cells from AC133-positive progenitor cells. *Blood* **95**, 3106-3112.
Gothert, J. R., Gustin, S. E., Van Eekelen, J. A., Schmidt, U., Hall, M. A., Jane, S. M., Green, A. R., Gottgens, B., Izon, D. J. and Begley, C. G. (2004). Genetically tagging endothelial cells in vivo: bone marrow-derived cells do not contribute to tumor endothelium. *Blood* **104**, 1769-1777.
Grunewald, M., Avraham, I., Dor, Y., Bachar-Lustig, E., Itin, A., Yung, S., Chimenti, S., Landsman, L., Abramovitch, R. and Keshet, E. (2006). VEGF-induced adult neovascularization: recruitment, retention, and role of accessory cells. *Cell* **124**, 175-189.
Hagedorn, M., Javerzat, S., Gilges, D., Meyre, A., de Lafarge, B., Eichmann, A. and Bikfalvi, A. (2005). Accessing key steps of human tumor progression in vivo by using an avian embryo model. *Proc. Natl. Acad. Sci. USA* **102**, 1643-1648.
Hamburger, V. and Hamilton, H. H. (1951). A series of normal stages in the development of the chick embryo. *J. Morphol.* **88**, 49-92.
Hillebrands, J. L., Klatter, F. A., Van Dijk, W. D. and Rozing, J. (2002). Bone marrow does not contribute substantially to endothelial-cell replacement in transplant arteriosclerosis. *Nat. Med.* **8**, 194-195.
Kennedy, L. J., Jr and Weissman, I. L. (1971). Dual origin of intimal cells in cardiac-allograft arteriosclerosis. *N. Engl. J. Med.* **285**, 884-887.
Kurz, H. and Christ, B. (1998). Embryonic CNS macrophages and microglia do not stem from circulating, but from extravascular precursors. *Glia* **22**, 98-102.
Kurz, H., Korn, J., Eggli, P. S., Huang, R. and Christ, B. (2001). Embryonic central nervous system angiogenesis does not involve blood-borne endothelial progenitors. *J. Comp. Neurol.* **436**, 263-274.
Larger, E., Marre, M., Corvol, P. and Gasc, J. M. (2004). Hyperglycemia-induced defects in angiogenesis in the chicken chorioallantoic membrane model. *Diabetes* **53**, 752-761.
La Rue, A. C., Lansford, R. and Drake, C. J. (2003). Circulating blood island-derived cells contribute to vasculogenesis in the embryo proper. *Dev. Biol.* **262**, 162-172.
Le Douarin, N. M. (1969). Particularités du noyau interphasique chez la caille japonaise (*Coturnix coturnix japonica*). Utilisation de ces particularités comme "marquage biologique" dans les recherches sur les interactions tissulaires et les migrations cellulaires au cours de l'ontogenèse. *Bull. Biol. Fr. Belg.* **103**, 435-452.
Lin, Y., Weisdorf, D. J., Solovey, A. and Hebbel, R. P. (2000). Origin of circulating endothelial cells and endothelial outgrowth from blood. *J. Clin. Invest.* **105**, 71-77.
Lippincott-Schwartz, J. and Fambrough, D. M. (1986). Lysosomal membrane dynamics: structure and interorganellar movement of a major lysosomal membrane glycoprotein. *J. Cell Biol.* **102**, 1593-1605.
Machein, M. R., Renninger, S., de Lima-Hahn, E. and Plate, K. H. (2003). Minor contribution of bone marrow-derived endothelial progenitors to the vascularization of murine gliomas. *Brain Pathol.* **13**, 582-597.
Montesinos, M. C., Shaw, J. P., Yee, H., Shamamian, P. and Cronstein, B. N. (2004). Adenosine A(2A) receptor activation promotes wound neovascularization by stimulating angiogenesis and vasculogenesis. *Am. J. Pathol.* **164**, 1887-1892.
Murray, P. D. F. (1932). The development *in vitro* of blood of the early chick embryo. *Strangeways Res. Lab. Cambridge* **111**, 497-521.
Navarro, M., DeRuiter, M. C., Carretero, A. and Ruberte, J. (2003). Microvascular assembly and cell invasion in chick mesonephros grafted onto chorioallantoic membrane. *J. Anat.* **202**, 213-225.
Pardanaud, L., Altmann, C., Kitos, P., Dieterlen-Lièvre, F. and Buck, C. (1987). Vasculogenesis in the early quail blastodisc as studied with a monoclonal antibody recognizing endothelial cells. *Development* **100**, 339-349.
Pardanaud, L., Yassine, F. and Dieterlen-Lièvre, F. (1989). Relationship between vasculogenesis, angiogenesis and haemopoiesis during avian ontogeny. *Development* **105**, 473-485.
Pardanaud, L., Luton, D., Prigent, M., Bourcheix, L. M., Catala, M. and Dieterlen-Lièvre, F. (1996). Two distinct endothelial lineages in ontogeny, one of them related to hemopoiesis. *Development* **122**, 1363-1371.
Parnot, C., Le Moullec, J. M., Cousin, M. A., Guedin, D., Corvol, P. and Pinet, F. (1997). A live-cell assay for studying extracellular and intracellular endothelin-converting enzyme activity. *Hypertension* **30**, 837-844.
Peichev, M., Naiyer, A. J., Pereira, D., Zhu, Z., Lane, W. J., Williams, M., Oz, M. C., Hicklin, D. J., Witte, L., Moore, M. A. S. et al. (2000). Expression of VEGFR-2 and AC133 by circulating human CD34$^+$ cells identifies a population of functional endothelial precursors. *Blood* **95**, 952-958.
Pudliszewski, M. and Pardanaud, L. (2005). Vasculogenesis and angiogenesis in the mouse embryo studied using quail/mouse chimeras. *Int. J. Dev. Biol.* **49**, 355-361.
Rajantie, I., Ilmonen, M., Alminaite, A., Ozerdem, U., Alitalo, K. and Salven, P. (2004). Adult bone marrow-derived cells recruited during angiogenesis comprise precursors for periendothelial vascular mural cells. *Blood* **104**, 2084-2086.
Risau, W. and Lemmon, V. (1988). Changes in the vascular extracellular matrix during embryonic vasculogenesis and angiogenesis. *Dev. Biol.* **125**, 441-450.
Ruzinova, M. B., Schoer, R. A., Gerald, W., Egan, J. E., Pandolfi, P. P., Rafii, S., Manova, K., Mittal, V. and Benezra, R. (2003). Effect of angiogenesis inhibition by Id loss and the contribution of bone-marrow-derived endothelial cells in spontaneous murine tumors. *Cancer Cell* **4**, 277-289.
Sabin, F. (1920). Studies on the origin of blood vessels and of red blood corpuscules as seen in the living blastoderm of chicks during the second day of incubation. *Contrib. Embryol. Carnegie Inst.* **9**, 214-262.
Seifert, R., Zhao, B. and Christ, B. (1992). Cytokinetic studies on the aortic endothelium and limb bud vascularization in avian embryos. *Anat. Embryol.* **186**, 601-610.
Shi, Q., Rafii, S., Wu, M. H., Wijelath, E. S., Yu, C., Ishida, A., Fujita, Y., Kothari, S., Mohle, R., Sauvage, L. R. et al. (1998). Evidence for circulating bone marrow-derived endothelial cells. *Blood* **92**, 362-367.
Sivan-Loukianova, E., Awad, O. A., Stepanovic, V., Bickenbach, J. and Schatteman, G. C. (2003). CD34+ blood cells accelerate vascularization and healing of diabetic mouse skin wounds. *J. Vasc. Res.* **40**, 368-377.
Stump, M. M., Jordan, G. L., Jr, Debakey, M. E. and Halpert, B. (1963). Endothelium grown from circulating blood or isolated intravascular Dacron hub. *Am. J. Pathol.* **43**, 361-372.
Takahashi, T., Kalka, C., Masuda, H., Chen, D., Silver, M., Kearny, M., Magner, M., Isner, J. M. and Asahara, T. (1999). Ischemia- and cytokine-induced mobilization of bone marrow-derived endothelial progenitor cells for neovascularization. *Nat. Med.* **5**, 434-438.
Tepper, O. M., Capla, J. M., Galiano, R. D., Ceradini, D. J., Callaghan, M. J., Kleinman, M. E. and Gurtner, G. C. (2005). Adult vasculogenesis occurs through in situ recruitment, proliferation, and tubulization of circulating bone marrow-derived cells. *Blood* **105**, 1068-1077.
Thomas, J. L., Pourquié, O., Coltey, M., Vaigot, P. and Le Douarin, N. M. (1993). Identification in the chicken of GRL1 and GRL2: two granule proteins expressed on the surface of activated leukocytes. *Exp. Cell Res.* **204**, 156-166.
Urbich, C. and Dimmeler, S. (2004a). Endothelial progenitor cells: characterization and role in vascular biology. *Circ. Res.* **95**, 343-353.
Urbich, C. and Dimmeler, S. (2004b). Endothelial progenitor cells functional characterization. *Trends Cardiovasc. Med.* **14**, 318-322.
Vajkoczy, P., Blum, S., Lamparter, M., Mailhammer, R., Erber, R., Engelhardt, B., Vestweber, D. and Hatzopoulos, A. K. (2003). Multistep nature of microvascular recruitment of ex vivo-expanded embryonic endothelial progenitor cells during tumor angiogenesis. *J. Exp. Med.* **197**, 1755-1765.
Vandenbunder, B., Pardanaud, L., Jaffredo, T., Mirabel, M. A. and Stéhelin, D. (1989). Complementary patterns of expression of c-ets 1, c-myb and c-myc in the blood-forming system of the chick embryo. *Development* **107**, 265-274.
Voswinckel, R., Ziegelhoeffer, T., Heil, M., Kostin, S., Breier, G., Mehling, T., Haberberger, R., Clauss, M., Gaumann, A., Schaper, W. et al. (2003). Circulating vascular progenitor cells do not contribute to compensatory lung growth. *Circ. Res.* **93**, 372-379.
Wong, T. S. and Ordahl, C. P. (1996). Troponin T gene switching is developmentally regulated by plasma-borne factors in parabiotic chicks. *Dev. Biol.* **180**, 732-744.
Yamashita, J., Itoh, H., Hirashima, M., Ogawa, M., Nishikawa, S., Yurugi, T., Naito, M., Nakao, K. and Nishikawa, S. (2000). Flk1-positive cells derived from embryonic stem cells serve as vascular progenitors. *Nature* **408**, 92-96.
Young, P. P., Hofling, A. A. and Sands, M. S. (2002). VEGF increases engraftment of bone marrow-derived endothelial progenitor cells (EPC) into vasculature of newborn murine recipients. *Proc. Natl. Acad. Sci. USA* **99**, 11951-11956.
Yurugi-Kobayashi, T., Itoh, H., Yamashita, J., Yamahara, K., Hirai, H., Kobayashi, T., Ogawa, M., Nishikawa, S., Nishikawa, S. and Nakao, K. (2003). Effective contribution of transplanted vascular progenitor cells derived from embryonic stem cells to adult neovascularization in proper differentiation stage. *Blood* **101**, 2675-2678.
Zentilin, L., Tafuro, S., Zacchigna, S., Arsic, N., Pattarini, L., Sinigaglia, M. and Giacca, M. (2006). Bone marrow mononuclear cells are recruited to the sites of VEGF-induced neovascularization but are not incorporated into the newly formed vessels. *Blood* **107**, 3546-3554.